Flow of two-dimensional crystals

Federico Ghimenti, Misaki Ozawa, and Giulio Biroli
Laboratoire de Physique de l'Ecole normale supérieure, ENS, Université PSL, CNRS, Sorbonne Université, Université Paris-Diderot, Sorbonne Paris Cité, Paris, France

Gilles Tarjus
LPTMC, CNRS-UMR 7600, Sorbonne Université, 4 Place Jussieu, 75252 Paris cedex 05, France
(Dated: September 8, 2022)

Below you find the plan of the article with already suggestions for the figures.

I. INTRODUCTION

Giulio and Gilles: Our motivation is to understand the behavior of solids at small shear stress: Do solids flow? The context we put forward is the Sausset et al paper and the one by Dasgupta et al.
This work investigate thoroughly this question for two-dimensional crystals.

Federico: **Previous literature**: Dislocation nucleation in the presence of an external strain has been observed in indented colloidal crystals [1]. Numerical simulations of solids sheared at a constant rate yield a power law relation between shear rate and viscosity [2, 3], and shear induced melting in system of particles with a short range repulsive r^{-12} interaction has been observed in numerical simulations [4, 5]: a coexistence between hexatic and liquid is observed at intermediate shear rate, while at high shear rates a steady state liquid phase is reported. we will mention these later.More exotic behavior are reported in a work on sheared colloidal crystals [6], where an oscillating process of melting and recrystallisation appears as the system is sheared. The dynamics of dislocations and their effect on stress relaxation has been studied as well [7–10], but the analysis is restricted to one or few annealed dislocations.

II. METHODS

We study dense monodisperse colloidal crystals in two-dimensions where hydrodynamic interactions and inertial effects can be neglected, and only pairwise short-range soft potential can be considered. We perform overdamped Langevin dynamics for the position $\mathbf{r}_i = (x_i, y_i)$ of each particle under external shearing [11]:

$$\zeta \frac{\mathrm{d}\mathbf{r}_i}{\mathrm{d}t} = -\sum_{j\neq i} \partial_{\mathbf{r}_i} v(\mathbf{r}_i - \mathbf{r}_j) + \dot{\gamma}\mathbf{e}_x y_i + \mathbf{f}_i, \qquad (1)$$

with $v(\mathbf{r}) = \frac{\epsilon}{2}(1 - r/d)^2\theta(d - r)$, where $\theta(x)$ is the step function. $\dot{\gamma}$ is the shear rate of the system. The thermal bath is described through the stochastic force $\mathbf{f}_i$, which is a Gaussian white noise with correlations, $\langle f_i^\alpha(t) f_j^\beta(t')\rangle = 2k_BT\zeta\delta(t - t')\delta_{ij}\delta_{\alpha\beta}$, where T is the temperature of the bath and k_B is the Boltzmann constant. We measure length in units of the diameter d, time in units of $\tau_0 = \zeta d^2/\epsilon$, and temperature in units of ϵ/k_B.

We study N harmonic disks in a square box with the area $V = L^2$, where L is the linear box length. The packing fraction ϕ of the system is set to $\phi = 1.0$, for which the system has a first-order hexatic-liquid transition at $T_m \simeq 0.006$ in thermal equilibrium without shearing ($\dot{\gamma} = 0$) [12]. To implement the external shearing, Lees-Edwards periodic boundary conditions are applied [13], and equations of motion are integrated through the Euler scheme. We measure the shear stress σ of the system by using the Irving-Kirkwood formula [13]. All quantities measured in this paper are obtained under the steady-state otherwise stated. We investigate a wide range of $\dot{\gamma}$ and T, which cover most of the relevant physics of two-dimensional crystal flows. We study $N = 900$, 3600, 14400, and 57600 to check finite size effects.

The phase diagram of the simulated model is presented in Fig. 1(a). As the temperature T and the shear rate $\dot{\gamma}$ are varied, the system enters three different regimes in the phase diagram. At smaller $\dot{\gamma}$ and T, we found plastic flow with free nucleated dislocations and hexatic quasi-long-range order (Regime I). The corresponding snapshot is shown in Fig. 1(b). Particles with 6 neighobrs are shown in white. Particles with 7 and 5 neighbors are shown in red and blue, respectivley. They form a dislocation. As $\dot{\gamma}$ or T is increased, a continuous transition to a regime where the dislocations are unbinded and free disclinations are nucleated (Regime II and corresponding snapshot in Fig. 1(c)). Finally, a cross-over to a laminar flow is observed as $\dot{\gamma}$ is further increased (Regime III and corresponding snapshot in Fig. 1(d)). In the subsequent sections, we will provide detailed characterizations of the three regimes.

III. SMALL SHEAR RATE REGIME: DO TWO DIMENSIONAL CRYSTALS FLOW?

A. Theoretical arguments and previous results

Giulio: Recall the argument of Bruinsma et al, and Sausset et al.

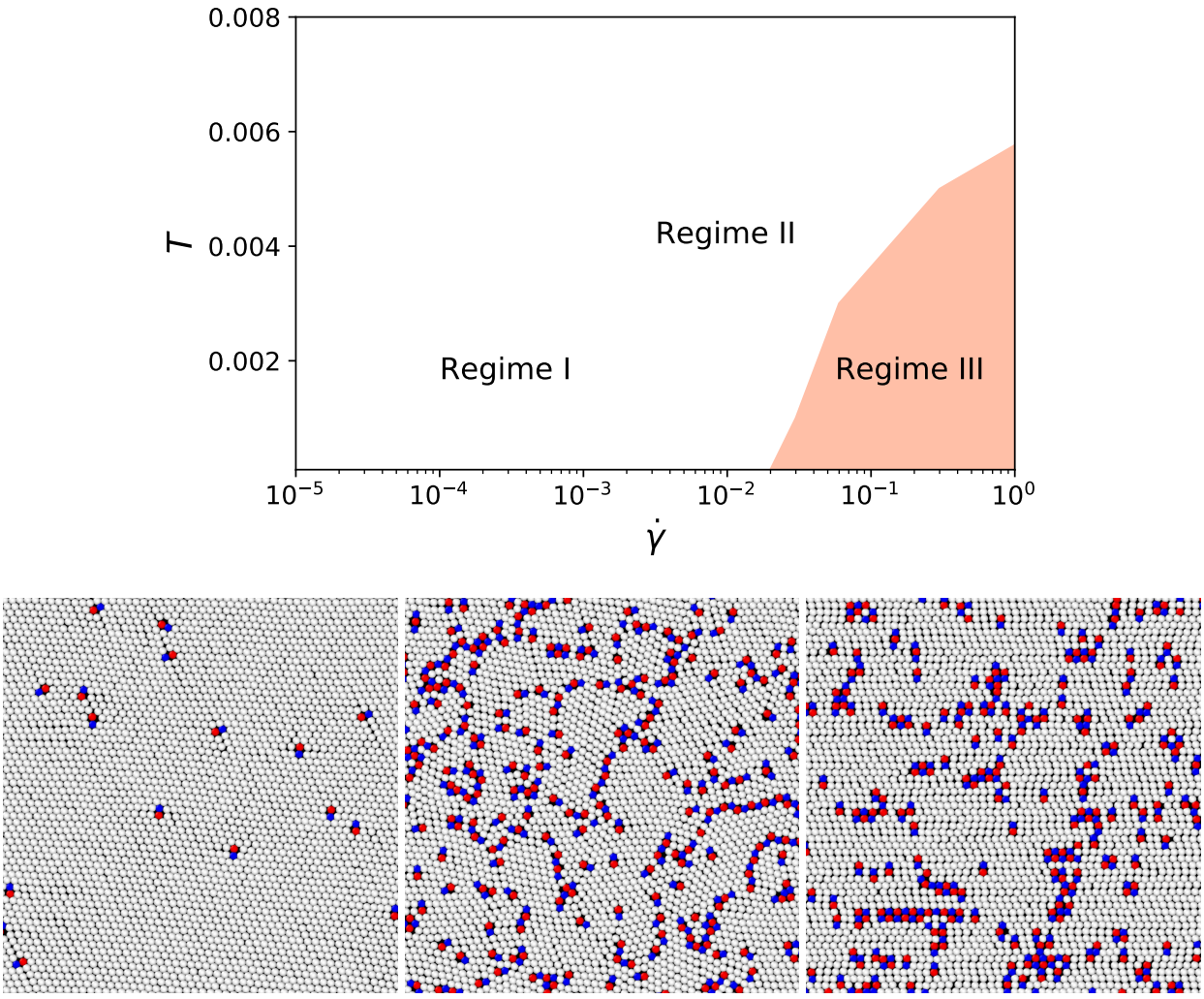

FIG. 1. (a): Phase diagram for the flow of a two-dimensional crystal in the plane of the shear rate $\dot{\gamma}$ and temperature T. In Regime I, plastic flow with free nucleated dislocations and hexatic quasi-long-range order (QLRO) are present. The corresponding snap shot is shown in (b). The theory of Sausset *et al.* applies to this regime [14]. Continuous transitions to Regime II showing the unbinding of disclinations are observed when $\dot{\gamma}$ is increased, or T is increased (see the corresonding snapshot (c)). Further increase of $\dot{\gamma}$ leads to laminar flow in Regime III (see aslo (d)).

B. Absence of yield-stress and dislocation unbinding

We first measure the shear stress σ at the steady-state as a function of the imposed shear rate $\dot{\gamma}$, encompassing more than three decades, as shown in Fig. 2(a). We vary the temperature T in a wide range from $T = 0.0001$ to 0.0080, which covers solid and liquid phases studied at $\dot{\gamma} = 0$. In particular, a frist-order hexatic-liquid transition temperature identified at $\dot{\gamma} = 0$ locates $T_m \simeq 0.006$ [12].

We now ask a fundamental question whether a two-dimensional crystalline solid flows at the infinitesimal stress, in other words, whether yield stress exists. The flow curves at lower temperatures, $T = 0.0010$ and 0.0010, show a plateau at smaller $\dot{\gamma}$ with apparent yield stress within our simulation time window. Instead, at intermediate temperatures, $T = 0.0030$ and 0.0050 (below T_m at $\dot{\gamma} = 0$), σ decreases steadily with decreasing $\dot{\gamma}$, as one can recognize more clearly in the zoomed-in plot in Fig. 2(b). These numerical data support the absence of the yield stress at $\dot{\gamma} \to 0$. We expect that σ for $T = 0.0001$ and 0.0010 also show a steady decrease at much lower $\dot{\gamma}$ outside our simulation range. As T is increased further, σ decreases rapidly, entering the Newtonian fluid regime ($T = 0.0080$).

We then plot the viscosity $\eta = \sigma/\dot{\gamma}$ in Fig. 2(c). At lower and intermediate temperatures, $T = 0.0001 - 0.0050$, we find a power-law divergence, $\eta \sim \dot{\gamma}^{-\alpha}$, at $\dot{\gamma}$, with $\alpha \approx ?? < 1$, as predicted by theory of Bruisma and Sausset. Moreover, η decreases with increasing T while keeping essentially the same scaling behavior. For higher

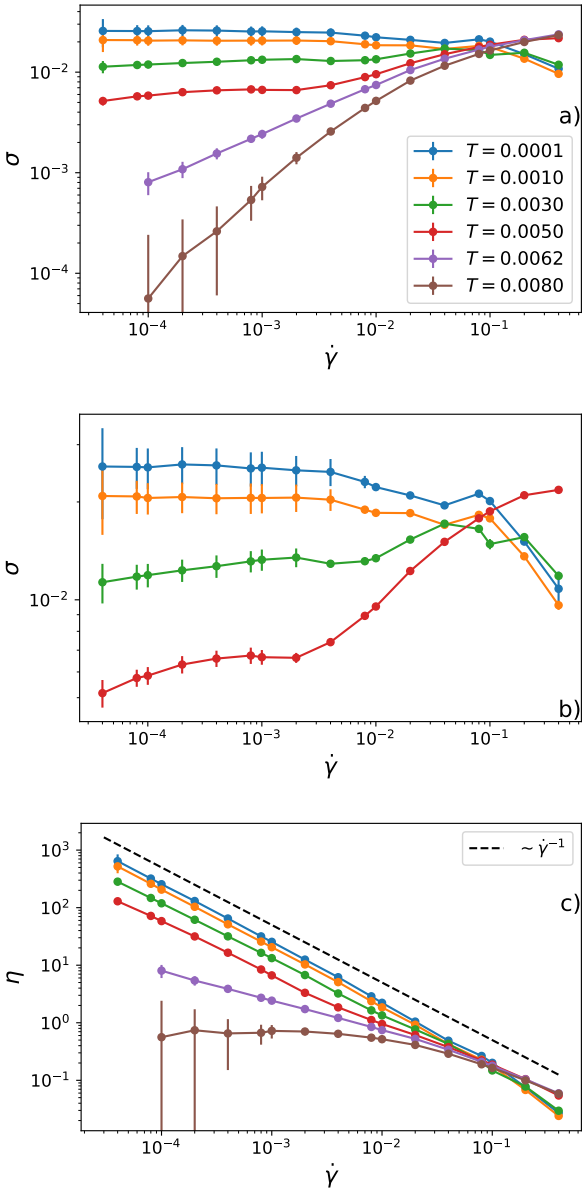

FIG. 2. Flow curves for a crystal of $N = 14400$ particles under shearing. (a): Shear stress σ versus the shear rate $\dot\gamma$ for several fixed temperatures. (b): Zoom-in plot of the panel (a) showing the absence of yield stress at $\dot\gamma \to 0$. (c): Viscosity $\eta = \sigma/\dot\gamma$ versus $\dot\gamma$. we can put $N = 3600$ and 57600 data as well.

temperatures ($T = 0.0080$), instead, η saturates toward a finite value, demonstrating a Newtonian fluid. We vary system size $N = 900$, 3600, and 14400 for measuring σ and η, and confirm that there is no noticiable finite size effect (see SI).

These numerical results, the absence of the yield stress and the divergence of viscosity, are fully consistent with the theoretical scenario mentioned above: A plastic flow is driven by free nucleated dislocations assisted by imposed stress (or shear rate). In this scenario, the nucleation rate increases with temperature, allowing for a higher density of dislocations, $\rho_{\rm disl}$, which provides, in turn, a faster relaxation of the shear stress and a lower viscosity, namely, $\eta \sim \rho_{\rm disl}$.

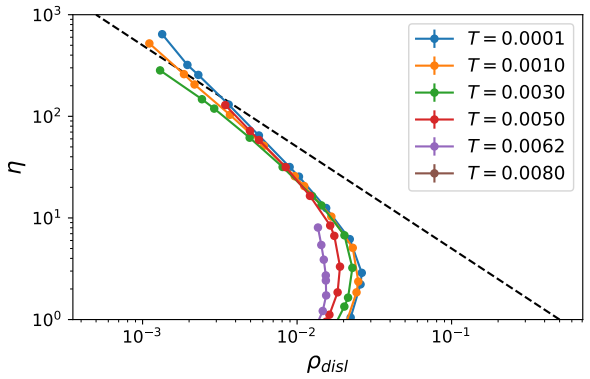

FIG. 3. Density of free dislocations, $\rho_{\rm disl}$, as a function of the shear rate $\dot\gamma$ (a) and the viscosity η (b) for a system of $N = 14400$ particles. $\rho_{\rm disl}$ at lower temperatures evolves in a power law fashion at smaller $\dot\gamma$ and larger η. The dashed straight line in (b) shows the scaling $\rho_{\rm disl} \sim \eta^{-1}$ predicted by the theory of Bruinsma *et al.* [15]

To test this prediction, in Fig. 3, we plot η as a function of $\rho_{\rm disl}$ determined numerically (see SI). Details on how the density $\rho_{\rm disl}$ is measured is explained in the SI. We find that numerical data at different temperatures are nearly superimposed at higher η (or higher $\dot\gamma$), and show asymptotically $\eta \sim \rho_{\rm disl}^{-1}$. Thus the viscosity divergence is govern by rarefraction of the deslocation dennsity as desribed by theory. At lower η (or lower $\dot\gamma$ regime), the data do not colapse and show a non-monotonic dependence. This is outside the theoretical scenario

For low shear rates, we confirm a power-law relation between $\rho_{\rm disl}$ and $\dot\gamma$ or η. The power-law breaks down at intermediate values of the shear rate where disclinations unbind, see Sec. IV B. The theory of Bruinsma *et al.* predicts that a scaling relation for the density of defects $\rho_{\rm disl} \sim \eta^{-1}$, while the slope of the curves in Fig. 3 is lower. We explain this difference as a precursor effect of the breakdown of the theory at intermediate shear rates.

Within our numerical accuracy, we cannot decide wihch theories are more appropriate.

IV. SHEAR-INDUCED TRANSITION FROM HEXATIC-LIKE TO LIQUID REGIMES

A paragraph to introduce the section and to refer to the phase diagram shown in the introduction.

A. Hexatic quasi long-range order at small shear stress

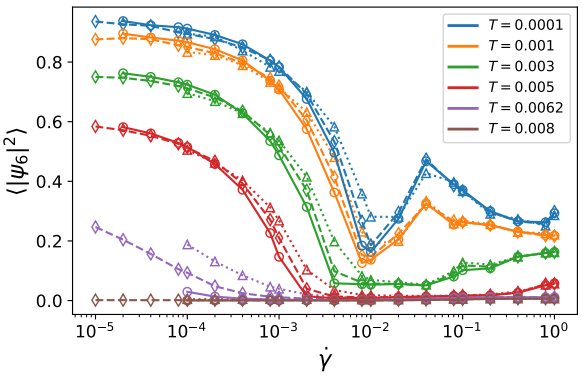

FIG. 4. Modulus global bond-orientational order parameters ψ_6 for various shear rates, temperatures and system sizes (circles with continuous lines: $N = 14400$; diamonds with dashed lines: $N = 3600$; triangles with empty lines: $N = 900$).

Gilles: Discuss/recap the physics of 2D crystals and discuss why one expects hexactic QLRO at small σ.

Federico:
Fig.4 shows the moduli of local and global bond-orientational order parameters $|\phi_6|$ and $|\psi_6|$ at various temperatures and shear rates. we will write the definitions Thermal vibrations and the presence of dislocations reduce the average value of the bond-orientational order parameters, which decrease slowly as the shear rate and temperature increase. The correlation function g_6 is studied in Fig.5, and at low shear rates a power-law decay is apparent: the nucleated dislocations traveling free through the crystal produce hexatic QLRO.

Because of the decay of g_6, in the thermodynamic limit the integral of ϕ_6 over the whole system should average to 0, and therefore one would expect $\psi_6 = 0$. The finite value of ψ_6 observed in this work is a finite size effect, as well as another peculiar phenomenon, the crystal rotation. If the system is small enough compared to the decay of g_6, the decorrelation of the bond-orientational order is weak, and an homogeneous rotation occur. The sample coherently change its orientation, and the global order parameter ψ_6 oscillates as shown in Fig. 6. If one plots the static structure factor $S(k)$, six peaks are observed at the corresponding vertices of the crystal's reciprocal lattice. These peaks rotate as the crystal is sheared, as shown in Fig. 7. Question: Is this hexatic phase like the equilibrium one? Or the critical properties are different? I don't remember where we stand/what we have on this the rotating we will refer experimental findings about rotation.

B. Transition

Federico: As the shear rate increases from low to intermediate values, dislocations proliferate, as one can see from Fig.??.

The abundance of defect leads to a steeper power law decay of g_6, which eventually breaks the KTHNY bound $g_6 \sim r^{-0.25}$, see Fig. 5. This phenomenon is associated with the appearance of free disclinations in the sample. To observe this phenomenon, we introduce a cut-off distance for defects identification. Once identified through the Voronoi tessellation procedure (see SI), we count the defect only if its distance from any other defect is bigger than a critical value d_c. While a change in the cut-off has little effect on $\rho_{dislocations}$ at low shear rates, the value of $\rho_{disclinations}$ is strongly affected by this choice, see SI. We track $p_{disclinations}$, the probability to have a non zero $\rho_{disclinations}$ during a single simulation run, for different cut-offs. When the value of the cut-off is high enough, we observe that $p_{disclination}$ is different from zero only above a critical value of $\dot{\gamma}$ that depends weakly on the value of the cut-off. Our result are showed here fr a representative value of the cut-off in Fig 8. This procedure allows one to clearly identify a continuous transition from a sheared crystal with only dislocations inside it to a sample where also disclinations appear, strengthening the decay of g_6 beyond the hexatic KTHNY prediction. Show and discuss the Figs on real space defects, and $\rho_{disclinations}$ vs $\dot{\gamma}$. Discussing that changing the cut-off one can clearly see that free disclinations are not present at low $\dot{\gamma}$ and then proliferate, hence the continuous transition.

V. CROSS-OVER TO LAMINAR FLOW

Federico: Upon further increase of $\dot{\gamma}$, the shear field dominates the dynamics of the system, and at the steady state state particle flow along bands parallel to the direction of shearing. This structure is apparent already from a look at the real space structure of the steady state, see Fig. **??**. A signature of a laminar disposition of the particles can also be seen from the radial distribution function $g(r)$ for various shear rates in Fig. 9 At the highest $\dot{\gamma}$ a series of ripples appear in the radial distribution function, signaling the presence of the laminar structure. For a given $\dot{\gamma}$, the ripples are less apparent for higher temperatures, suggesting that the laminar flow results from a competition between the shear field and thermal fluctuations in the sample. Dynamics at this regime depends on dynamical rule. Dynamics with inertia generates liquid structure (not shown), instead of laminar, which is consistent with previous lieterature. We will mention the Grest paper.

VI. CONCLUSION

Giulio and Gilles: We can recap here the main motivation of our work, what we found, and the perspectives to

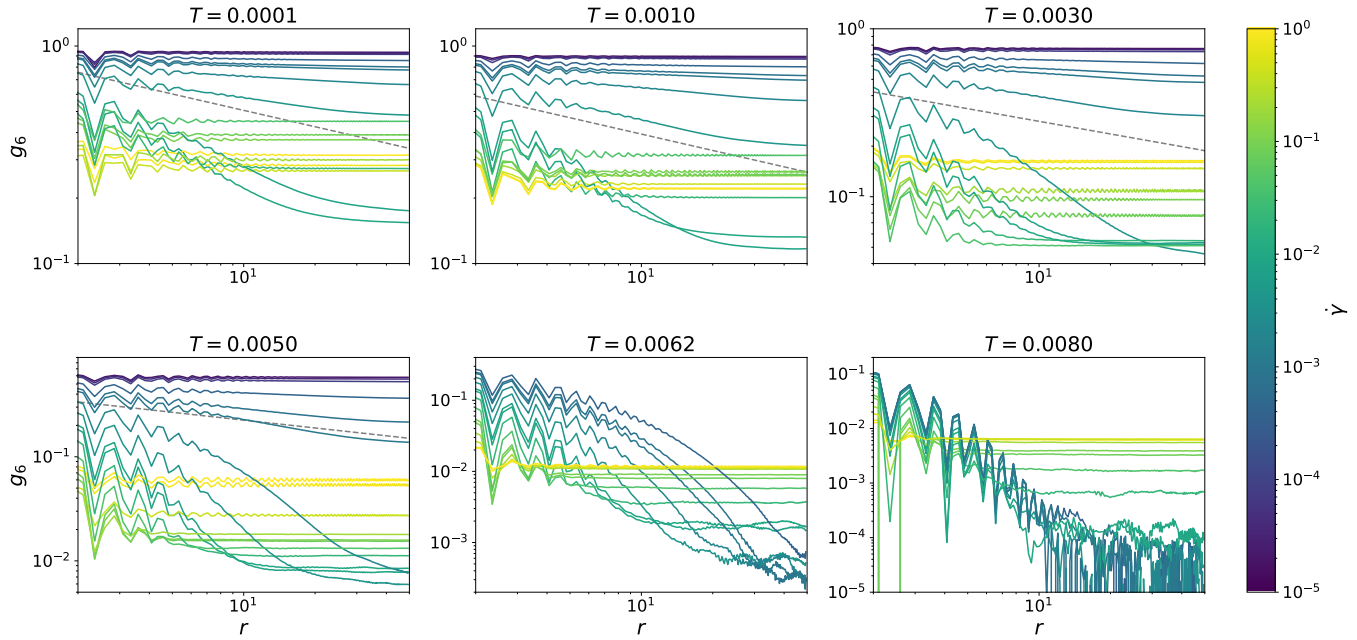

FIG. 5. Bond-orientational correlation function $g_6(r)$ for a system of 14400 (continuous line) and 3600 (dotted lines) particles I do not see a finite size effect.. The gray lines in the background represent the bound imposed by the KTHNY theory, $g_6 \sim r^{-0.25}$. A power law decay can be seen in the low shear rate regime, thus establishing the presence of hexatic QLRO in Regime I. The gray lines in the background represent the bound imposed by the KTHNY theory, $g_6 \sim r^{-0.25}$. This bound is violated when disclinations unbind, signaling the continuous transition to regime II.

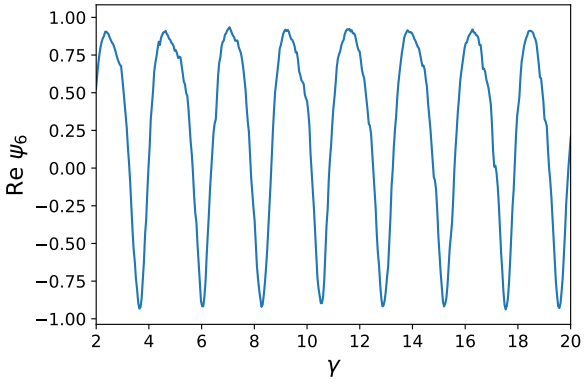

FIG. 6. Oscillations in the real part of the global orientational bond-order parameter ψ_6 as a function of the shear deformation γ for the rotating crystal ($N = 3600$, $T = 0.0001$ and $\dot{\gamma} = 5 \cdot 10^{-4}$). The oscillations reach values close to 1 and -1, signaling the coherence of the rotation.

address the same issue ("do solids flow?") in more general contexts, e.g. 3D crystals, 2D glasses, etc.

Discussion: similarity/difference with active cases

Appendix A: Dislocation

Explain how to define dislocation and compute its density.

Appendix B: Bond-orientational order parameters

Explain the definition of the bond-orientational order.

[1] P. Schall, I. Cohen, D. A. Weitz, and F. Spaepen, Visualizing dislocation nucleation by indenting colloidal crystals, Nature **440**, 319 (2006).

[2] W. G. Hoover, A. J. Ladd, and B. Moran, High-strain-rate plastic flow studied via nonequilibrium molecular dynamics, Physical Review Letters **48**, 1818 (1982).

[3] A. J. Ladd and W. G. Hoover, Plastic flow in close-packed crystals via nonequilibrium molecular dynamics, Physical Review B **28**, 1756 (1983).

[4] T. Weider, M. Glaser, H. Hanley, and N. Clark, Shear-induced melting of two-dimensional solids, Physical Review B **47**, 5622 (1993).

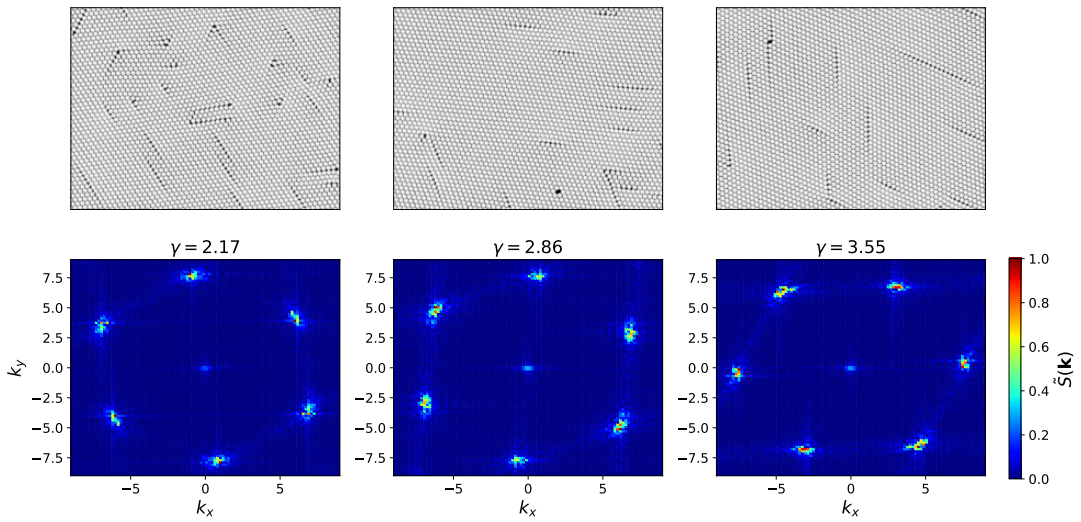

FIG. 7. Crystal rotation in real space (top) and in Fourier space (bottom) through the motion of the six hexagonal peaks of the rescaled static structure factor $\tilde{S}(k)$. Definition Measurements are taken for a system of 3600 particles at $T = 0.0001$ and $\dot{\gamma} = 5 \cdot 10^{-4}$, as the one of Fig. 6.

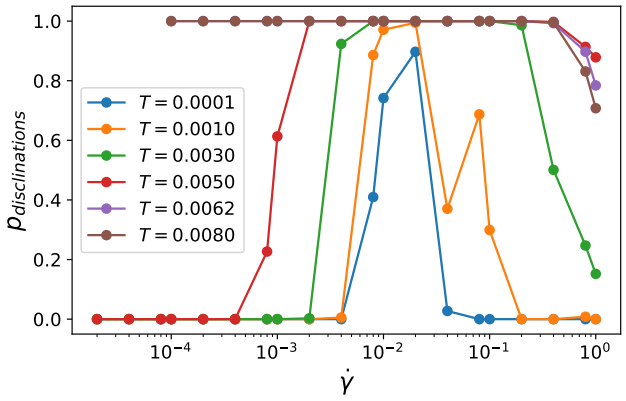

FIG. 8. Probability to find at least a disclination in the system at the steady state, $p_{disclinations}$ as a function of temperature and shear rate. The value of $\dot{\gamma}$ at which $p_{disclinations}$ departs from 0 is used to identify the transition from regime I to regime II.Ideally, we wish to increase the statistics for $T = 0.0010$ around $\dot{\gamma} = 0.1$

[5] J. Delhommelle, Simulations of shear-induced melting in two dimensions, Physical Review B **69**, 144117 (2004).

[6] E. J. Stancik, A. L. Hawkinson, J. Vermant, and G. G. Fuller, Dynamic transitions and oscillatory melting of a two-dimensional crystal subjected to shear flow, Journal of rheology **48**, 159 (2004).

[7] K. Kaski, A. Kuronen, and M. Robles, Dynamics of dislocations in a two-dimensional system, in *Computer Simulation Studies in Condensed-Matter Physics XIV* (Springer, 2002) pp. 12–26.

[8] N. Bailey, J. Sethna, and C. Myers, Dislocation mobility in two-dimensional lennard–jones material, Materials Science and Engineering: A **309**, 152 (2001).

[9] M. Popova, Y.-L. Shen, and T. A. Khraishi, Atomistic simulation of dislocation interactions in a model crystal subjected to shear, Molecular Simulation **31**, 1043 (2005).

[10] Y.-L. Shen, On the atomistic simulation of plastic deformation and fracture in crystals, Journal of materials research **19**, 973 (2004).

[11] A. Ikeda, L. Berthier, and P. Sollich, Unified study of glass and jamming rheology in soft particle systems, Physical review letters **109**, 018301 (2012).

[12] M. Zu, J. Liu, H. Tong, and N. Xu, Density affects the nature of the hexatic-liquid transition in two-dimensional melting of soft-core systems, Physical review letters **117**, 085702 (2016).

[13] M. P. Allen and D. J. Tildesley, *Computer simulation of liquids* (Oxford university press, 2017).

[14] F. Sausset, G. Biroli, and J. Kurchan, Do solids flow?, Journal of Statistical Physics **140**, 718 (2010).

[15] R. Bruinsma, B. Halperin, and A. Zippelius, Motion of defects and stress relaxation in two-dimensional crystals, Physical Review B **25**, 579 (1982).

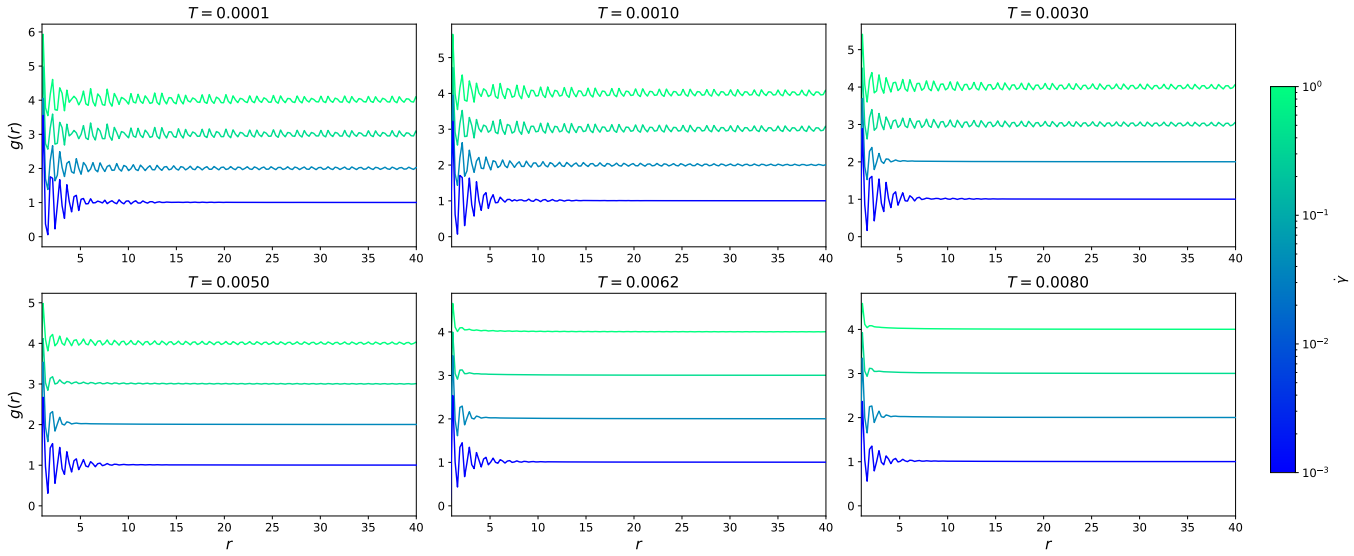

FIG. 9. Plot of the modulus of the shifted radial distribution function $g(r)$ for a system of $N = 14400$ particles through the flow. Oscillatios at small value of r disappears when passing from low to intermediate shear rates, while at the highest shear rates ripples appear, signaling the onset of laminar flow.